Design for a second-generation proton storage ring at LAMPF

E. P. Colton
Los Alamos National Laboratory
Los Alamos, NM 87545
USA

ABSTRACT: A conceptual design is presented for a second-generation proton storage ring complex at LAMPF. The facility would consist of two stacked racetrack-shaped machines. These machines would deliver a 1.2-mA beam of 1.6-GeV protons at 48 Hz. The pulse length would be 1.75 μsec which represents a time compression of 570.

1. Introduction

There is some local interest for a 1.6-GeV proton storage ring (PSR) which will deliver nominally 2 MW of beam power at 48 Hz. The design for the present PSR is just 80 kW so the improvement is a factor of ~25. The 1.6-GeV kinetic energy would be obtained from an add-on linac to LAMPF. The flux requirement is 1.5×10^{14} ppp at 48 Hz; the beam would be sent alternately to neutron production, and neutrino production experiments, respectively. These facilities would each operate at 24 Hz.

This request can be met by using two stacked rings which are respectively fed with two successive LAMPF macropulses. Each ring would store 7.5×10^{13} protons. Thus, 96 of the 120 LAMPF macropulses normally available in 1 sec would be devoted to these ends. Additionally, the present H^- source would have to be upgraded by a factor of two. Protons would be fast extracted in a single turn from each ring and sent to the experiments in box-car fashion. The pulse length would be 1.75 μsec, so the time compression is a factor of ~570. There are two constraints which must be met: (1) The slow losses which occur in the Los Alamos Proton Storage Ring (PSR) cannot take place in these rings.[1] (2) It is necessary to store beam in one of these rings for up to 8 msec, so the rings must be stable against coherent instability. In view of these

requirements, it appears to me that certain steps have to be taken—they are spelled out below.

1. The injection must be direct H^- to H^+ in a stripping foil instead of the two-step process used in the PSR. The stripping magnet introduces extra beam divergence in the bend plane. The lack of control over the neutral beam is another negative aspect.
2. The injected H^- beam should be matched to the machine in 6-D phase space. We need to limit the injected dp/p, and to stabilize the position of the beam at the foil in x-x' and y-y' phase space.
3. We need to choose an aperture large enough to contain the tails of the beam to the 99.9% level. Collimation schemes have to effectively restrict losses to the 100 nA level locally. Mainly, we are looking to absorb protons scattered out of the normal acceptance by large-angle scatters in the stripping foil.
4. Effective H^0 and H^- dumps should be provided to remove partially stripped or unstripped particles.
5. Efforts should be made to reduce the number of foil traversals for circulating protons. These include beam bumping, transverse painting, x-y mixing by means of skew quadrupoles, etc. The foil should be positioned at a beam waist with small β^*.
6. The machines should have long straight sections for injection, extraction and rf cavities.
7. We need to maintain a clean kicker gap for lossless extraction.
8. The maximum transverse space-charge tune shift $-dQ_y$ should not exceed 0.15. This requirement stipulates the beam core emittance.
9. With regard to coherent instabilities, we should endeavor to reduce the peak currents seen in the PSR, as well as maintain a significant dp/p width; this may be difficult to achieve with conventional rf systems. We really need to make a smooth vacuum chamber with gradual transitions.
10. Sextupole magnets should be included for chromaticity control, but their use should not reduce the ring admittance to below 1000 mm-mr.

The machine requirements have been met in a first-order design which is the subject of the remainder of this report. The design layout is shown

in Fig. 1. The shape is that of a near racetrack. The four bend sections are 90° bend achromats. The two short straight sections each contain fast extraction systems. The rf cavity is located in a dispersion free zone. The long straight section containing the injection area includes a special injection chicane, the stripping foil, an H^-/H^0 dump, two orbit bumpers, and two halo collimators. All of these are discussed below.

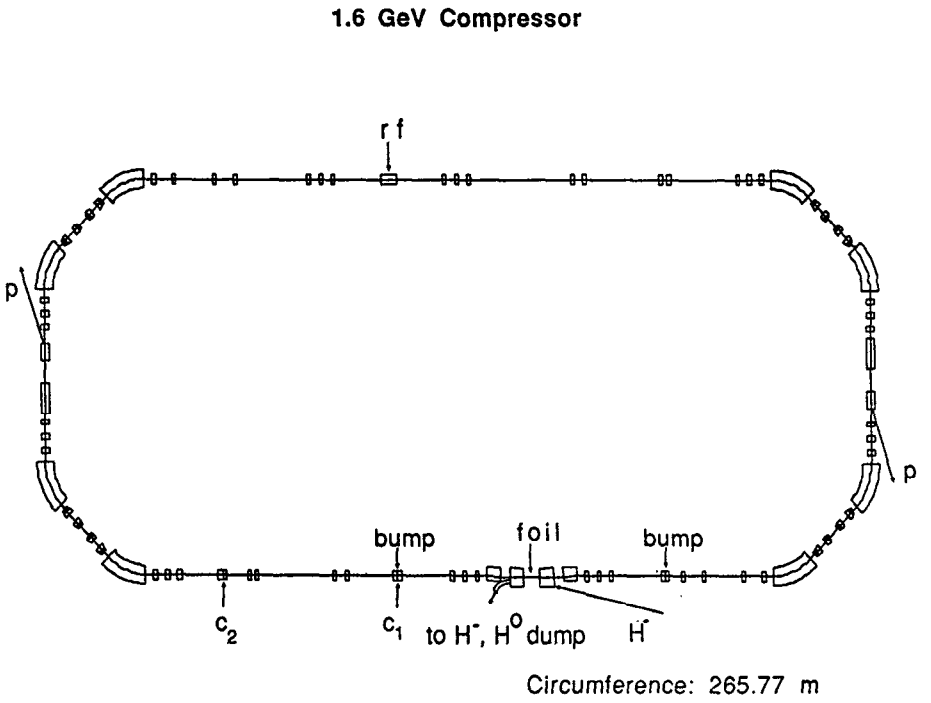

Fig. 1. Plan view layout of the new compressor rings.

Table I lists the parameters for the designed machines. The revolution frequency is 1.048 MHz, so the revolution time is 954 nsec. The pulses from the two rings will be extracted sequentially and sent in box-car fashion to the experimental areas. Allowing for a kicker gap of about 150 nsec, we would expect a final delivered pulse length of 1750 nsec (800 + 150 + 800).

In Section 2, I discuss the lattice design. In Section 3, I explain the mechanics of beam transfers. Collimation is briefly discussed in Section 4. The rf system is treated in Section 5. The subject of coherent instabilities is treated in Section 6. Concluding remarks are given in Section 7.

Table I. Machine Parameters

Kinetic Energy	1.6 GeV
Average Current Delivered	1.2 mA
Repetition Rate	48 Hz
	(24 to produce spallation neutrons)
	(24 to produce neutrinos)
Circumference	265.77 m
Protons per Pulse	1.5×10^{14}
Number of Rings/Superperiods	2/2
Circulating Current/Ring	12.6 A
Revolution Frequency	1.048 MHz
Number of Turns Injected	1048
Betatron Tunes Q_x, Q_y	5.23, 4.23
Chromaticity Q'_x, Q'_y	−7.32, −6.76
Transition Gamma γ_t	8.19

2. Lattice Design

The machine lattice functions across half the machine are depicted in Fig. 2(a); the maximum dispersion is 5.1 m in the center of an achromat. The β^* is 3.0 m at the stripping foil location. The beam halfwidths are shown in Fig. 2(b). These sizes were calculated using the expressions

$$x = \sqrt{\beta_x \varepsilon_x} + \left|\eta_x \frac{dp}{p}\right| \quad \text{and} \quad y = \sqrt{\beta_y \varepsilon_y} \qquad (2.1) \text{ and } (2.2)$$

with $\varepsilon_x = \varepsilon_y = 100$ mm-mr and $dp/p = \pm 0.003$. These values were obtained from a study of the injection process. The maximum vertical beam size in the dipoles is of order ± 35 mm. The betatron tunes for the whole machine are $Q_x = 5.23$ and $Q_y = 4.23$. The uncorrected chromaticities $dQ_x/dp/p = -7.32$ and $dQ_y/dp/p = -6.76$. The transition gamma $\gamma_t = 8.19$ so $\eta = \gamma_t^{-2} - \gamma^{-2} = -0.1217$.

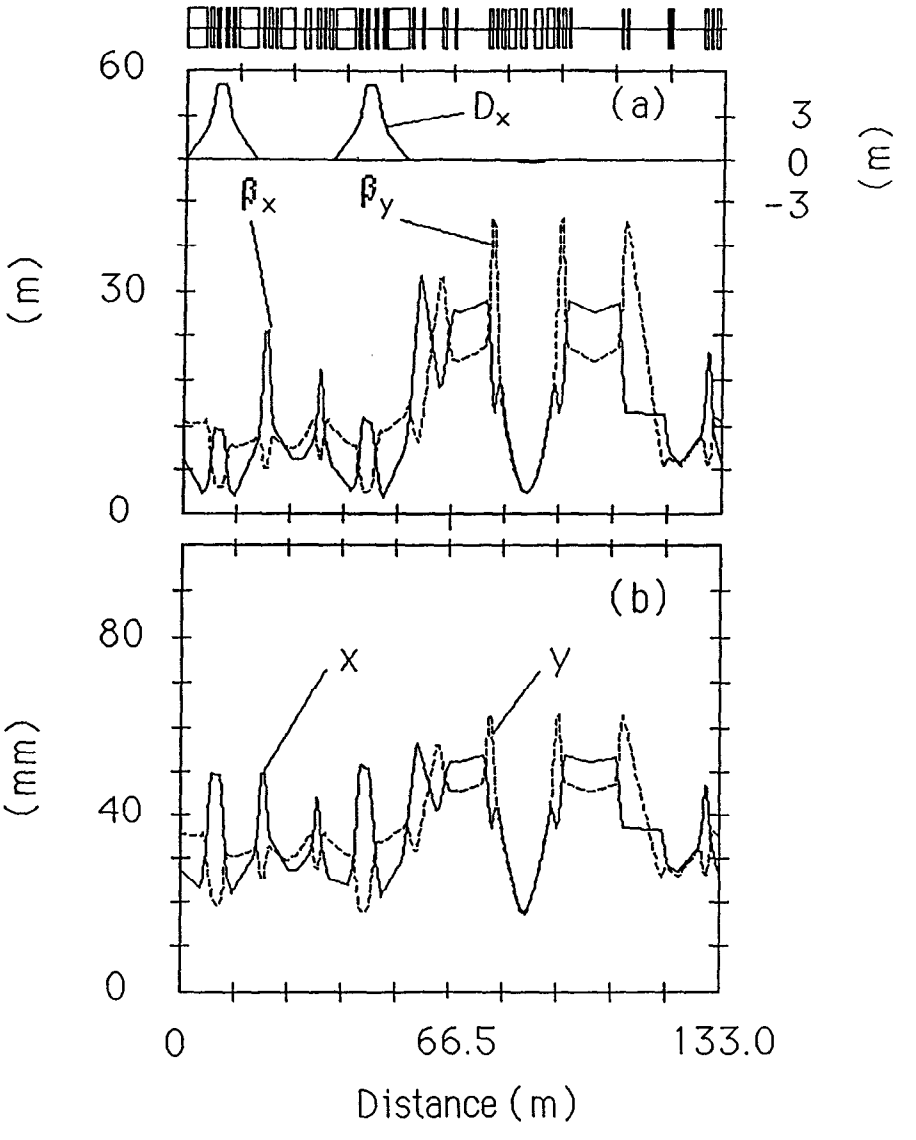

Fig. 2. (a) Machine lattice functions for 1 superperiod; (b) half beamwidths calculated using Eqs. (2.1) and (2.2). The emittances ε_x and ε_y are both 100 mm-mr and $dp/p = 0.003$.

3. Beam Transfers

A. H^- Injection

The ring injection takes place via the process $H^- \rightarrow H^+$ in a 250-$\mu g/cm^2$ carbon stripping foil. A plan view of the injection region is shown in Fig. 3; the four dipoles in the center translate the proton beam 171.5 mm to beam left of center at the stripping foil location (call this the center). The two fast orbit bumpers are separated by 180° in horizontal betatron phase—they serve to further displace the translated proton beam at the foil. The bump starts out at 20 mm left of center and reduces to 10 mm during the 1-msec injection period (this time corresponds to 1050 turns). After the injection the bumps are rapidly reduced to zero. Referring to Fig. 3, the H^- are injected into the second dipole and are nominally placed at 25 mm beam left of center, and on axis vertically.

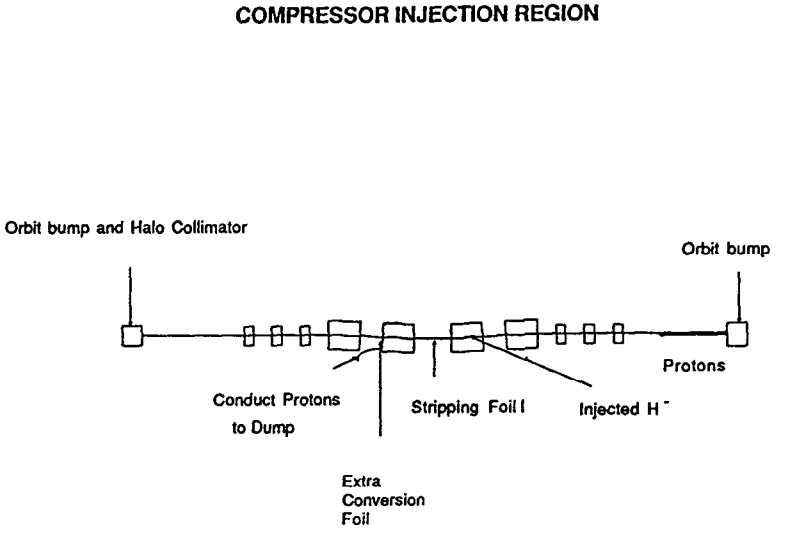

Fig. 3. Plan view of the H^- injection region.

Figure 4 shows a closeup plan view of the circulating proton and injected H^- beams in the region of the four dipole chicane. Unstripped H^- or partially stripped H^0 will exit the third dipole displaced to the outside of the proton beam; they will pass through another stripping foil, so as to convert to protons, and then be conducted away to a dump.

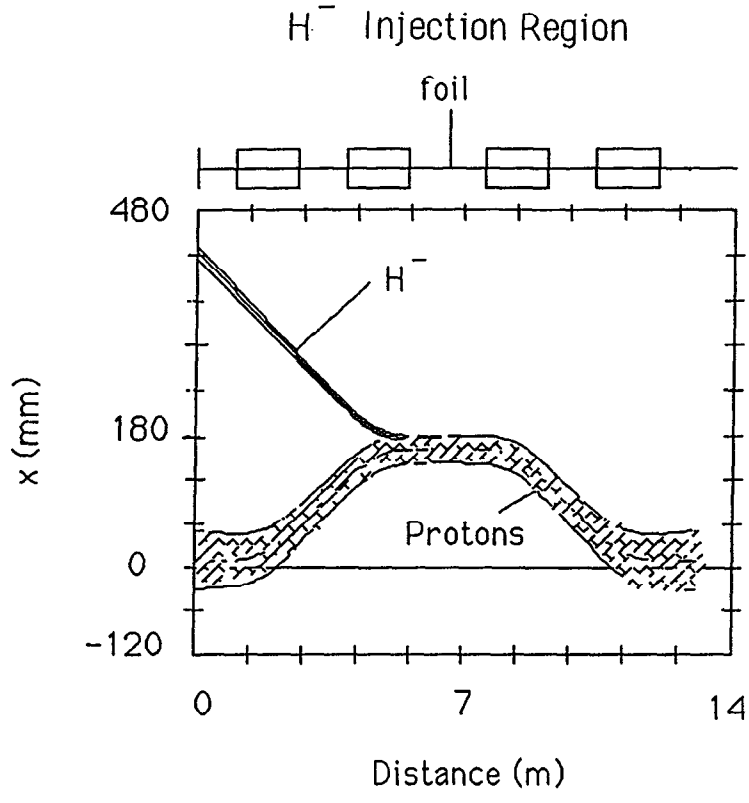

Fig. 4. Circulating proton and injected H^- beam envelopes within the four-dipole injection chicane. The proton beam geometric emittance is 100 mm-mr. The H^- injected emittance is of order 2–3 mm-mr.

B. Fast Extraction

Beam is extracted from each ring in a single turn and sent in box-car fashion to the experimental targets. Timewise, first one ring is filled in 1 msec and the second ring is filled 1/120 sec later. They are fast extracted together (separated by one revolution time). These processes are repeated 48 times per sec. A plan view layout of the extraction section is shown in Fig. 5. A 3.5-m ferrite kicker displaces the protons into the field region of a 1.5-m d.c. septum magnet from which they are conducted to the appropriate experimental area. Referring to Fig. 1, beam is extracted on alternate pulses from the two extraction sections and sent to the respective experimental targets at 24 Hz.

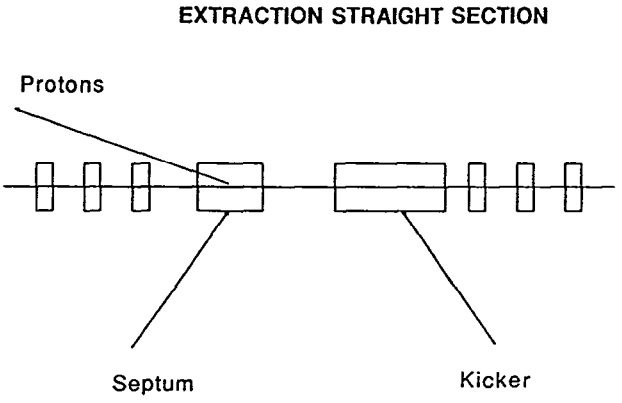

Fig. 5. Plan view of extraction straight section.

The horizontal beam envelopes in the extraction straight section are shown in Fig. 6; both the circulating and extraction envelopes are shown for an emittance of 100 mm-mr.

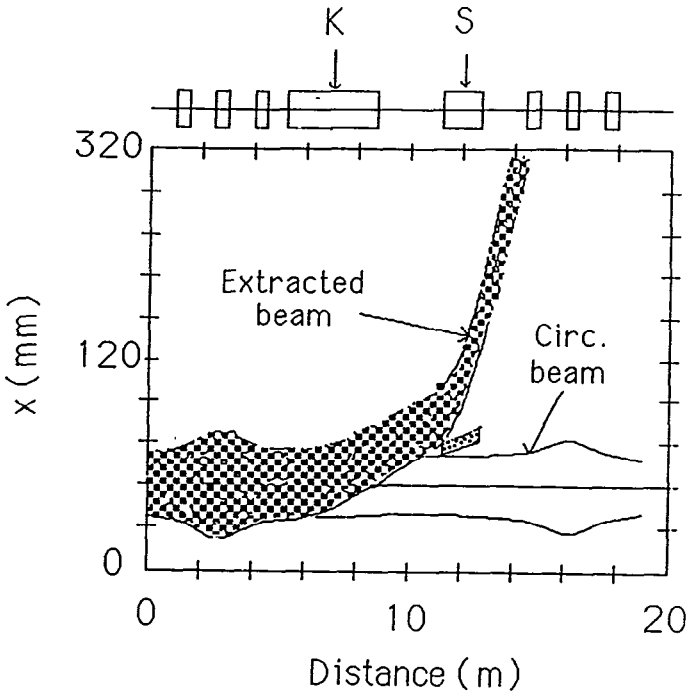

Fig. 6. Circulating and extracted proton beam envelopes in the extraction section. The emittance is 100 mm-mr.

4. Collimation

The injection foil is positioned offset to the outside of the machine to reduce the number of repeated proton traversals. These traversals cause the rms transverse emittance to grow by an amount $\beta^*\theta^2 fN(t)/2$ where β^* is the beta function at the foil, θ is the rms scattering angle for a single traversal, and $fN(t)$ is the number of foil traversals in N turns up to time t. To minimize the emittance growth we designed for $\beta^* = 3.0$ m at the foil and we try to reduce the probability for a traversal (f) by locating the foil edge close to the injected H^- beam spot. In fact, rms emittance growth due to foil scattering is only a few percent.

Of more concern are the large angle scatters due to nuclear or single coulomb scattering in the thin stripping foil. The largest angle we can reasonably expect to contain is about 2 mr. The probability for even larger scatters is $\sim 7 \times 10^{-6}$. If we roughly take 25 traversals for the average proton, then we would expect for 600 μA

$$\text{loss} = 600 \times 10^{-6} \times 25 \times 7 \times 10^{-6} = 105 \text{ nA} \ . \tag{4.1}$$

This loss would activate each machine downstream of the foil. We plan to quickly absorb these large angle scatters in the downstream collimators C_1 and C_2 (see Fig. 1). The collimators are strategically placed 90° and 180° in betatron phase downstream of the stripping foil, respectively. Some adjustment to the actual design would be necessary since an orbit bump magnet is coincident with C_1.

5. Rf System

The function of the rf system is to (i) maintain a longitudinal gap in the beam for lossless extraction and (ii) to produce enough relative momentum spread to keep the circulating protons coherently stable. The average circulating current is 12.6 amperes in each ring at full intensity. With a fundamental rf system, bunching will occur and the peak currents can be expected to rise to over 40 amperes; this will surely result in coherent instability and beam loss. For these rings I suggest use of the rf waveform shown in Fig. 7. The rf voltage is composed of the fundamental plus four harmonics

$$V(\phi) = V_0 \sum_{i=1}^{5} V_i \sin(i\phi) \tag{5.1}$$

with the indicated values for V_i. The voltages on the end act like repulsive barriers to the beam, hence the name barrier bucket. This waveform should maintain a gap in the beam. However, little or no increase in the dp/p occurs. We obtain larger dp/p values by just sweeping the energy of the injected beam in the last linac module. This sweeping is done sinusoidally with two oscillations over the 1 msec injection period.

A simulation has been performed in order to demonstrate the viability of the method. Beam was injected uniformly in rf phase ϕ for $|\phi| \leq 2.4$ radians—this corresponds to populating ~146 microbunches of the 192 possible. The dp/p were generated in a Gaussian fashion with $\sigma_p/p = 0.05\%$. During injection, the central value of the dp/p varied sinusoidally with turn number t as $0.002 \sin(2\pi t/525)$ (in absolute units). The rf voltage of the fundamental $V_0 * V_1 = 3.5$ kV, so the peak voltage of the waveform shown in Fig. 7 was 16.9 kV. The projections of ϕ and dp/p are given in Figs. 8(a) and 8(b), respectively. The gap is maintained in Fig. 8 and the rms ϕ width is unchanged from the injected value. The FWHM of the dp/p distribution is of order 0.5%.

The required rf voltages are relatively modest at the fundamental and its four higher harmonics. Perhaps two cavities will be required. The design can be similar to the PSR cavity with its very low R/Q, so beam loading should not be a problem. The effects of longitudinal space charge will be to decrease the action of the rf cavity, i.e., to fill in the extraction gap. Increased rf voltage is necessary to compensate this effect.

6. Beam Stability

A. Space-Charge Tune Shift

The space-charge tune shift is given by

$$|\Delta Q_y| = G_y \frac{2.4 \text{ mm} - \text{mr}}{\varepsilon_N} \frac{N}{10^{13}} \frac{F_y}{B\beta\gamma^2} \tag{6.1}$$

where G_y is a form factor depending upon the x-y spatial distribution, ε_N is the normalized vertical emittance which contains 87% of the beam, and N is the number of circulating protons. The remaining term is approximated by

$$\frac{F_y}{B\beta\gamma^2} \sim \frac{1.02}{B\beta\gamma^2} + 0.045\beta \tag{6.2}$$

where B is the bunching factor, $\beta = pc/E$, and $\gamma = E/moc^2$.

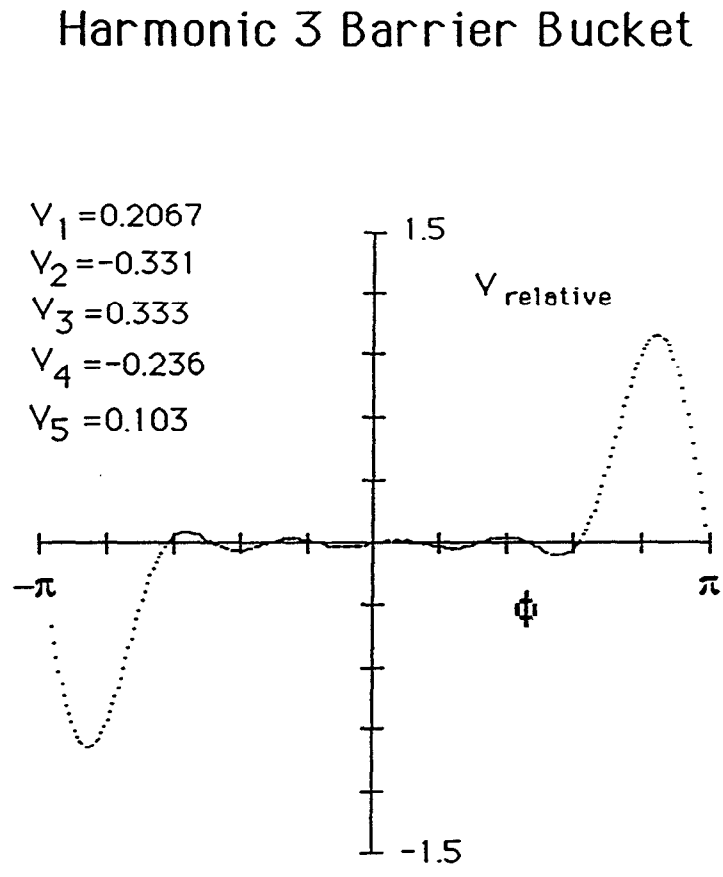

Fig. 7. Proposed rf waveform. The voltage is given by Eq. (5.1).

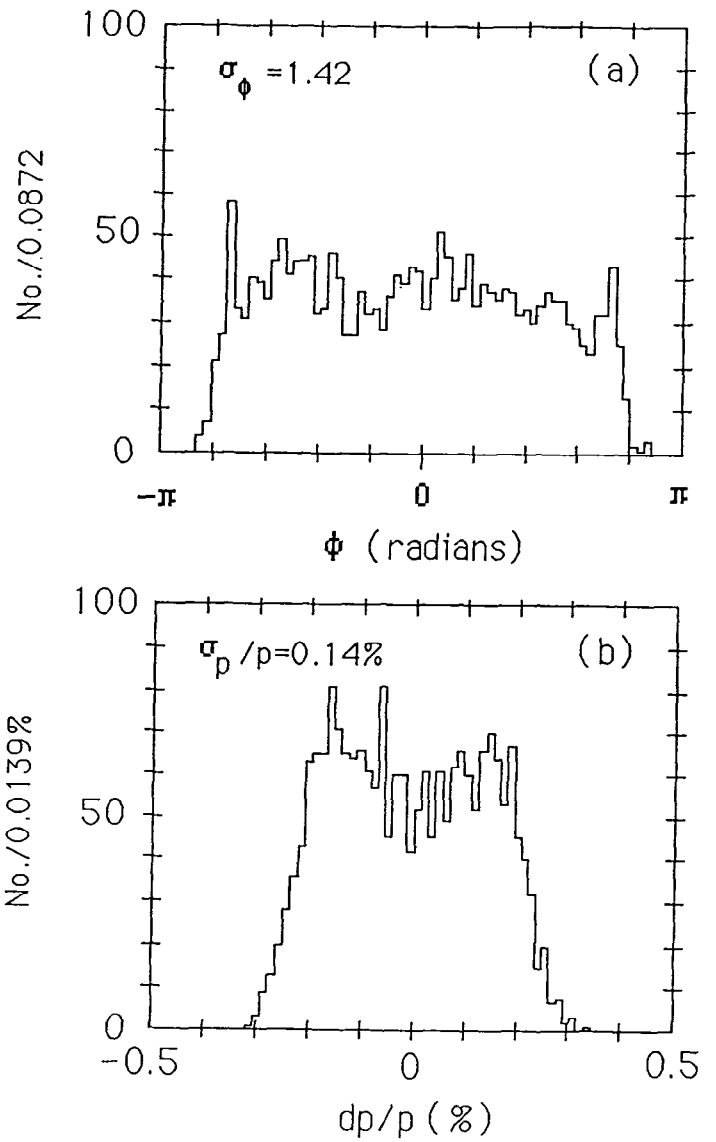

Fig. 8. *Rf simulation results for 1050 turns of injection.*

We pessimistically take $G_y = 2$ corresponding to a 2D Gaussian distribution. Next, ε_N is given by $\varepsilon_y \beta\gamma$ and we use $\varepsilon_y = 40$ mm-mr as determined in the injection simulations. I assume $N = 7.5 \times 10^{13}$ and a bunching factor $B = 0.65$. With these choices the space-charge tune shift is computed to be $|\Delta Q_y| = 0.098$.

B. Coherent Stability

The major coupling impedances are imaginary and due to space charge. They are

$$\frac{Z_\ell}{n} = \frac{i}{2}\frac{Z_0}{\beta\gamma^2}\left(1 + 2\ell n\frac{b}{a}\right) \tag{6.3}$$

where Z_0 is the impedance of free space, $Z_0 = 377$ ohms, and b/a is the ratio of beam pipe to beam radius $b/a \sim 2.67$. We obtain $Z_\ell/n = i82\Omega$. The transverse

$$Z_\perp = \frac{iRZ_0}{\beta^2\gamma^2}\left(\frac{1}{a^2} - \frac{1}{b^2}\right) = i\,2.4 \times 10^6\ \Omega/\text{m}\ . \tag{6.4}$$

I chose $a = 0.03$ m and $b = 0.08$ m. The average circulating current $I = 12.6$ amperes and the peak $\hat{I} = 19.4$ amperes for the rf system contemplated.

The test for longitudinal stability

$$\left(\frac{dp}{p}\right) \geq \left[\frac{\hat{I}}{\beta^2|\eta|E}\left|\frac{Z_\ell}{n}\right|\right]^{1/2} \tag{6.5}$$

where $\eta = \gamma_t^{-2} - \gamma^{-2} = -0.1218$.

I find $(dp/p)_{\text{FWHM}} \geq 0.24\%$. This is easily satisfied by our beam with $(dp/p)_{\text{FWHM}} \sim 0.5\%$ so the beam will be longitudinally stable.

The test for transverse stability

$$|Z_\perp| \leq 4\frac{\beta E}{\hat{I}}\frac{Q_y}{R}\left[(n - Q_y)\eta + \frac{dQ_y}{dp/p}\right]\left(\frac{dp}{p}\right)_{\text{FWHM}} \tag{6.6}$$

results in

$$|Z_\perp| \leq 0.2395 \times 10^6[(n - 4.23) \times 0.12 + 6.75]$$

If we use $|Z_\perp| = 2.4 \times 10^6\ \Omega/\mathrm{m}$, then we find the machine is stable for $n > 31$ or frequencies $f > 32.5$ MHz. Below this frequency the machine is unstable with a growth rate given by

$$\frac{1}{\tau} = \frac{Ic}{4\pi Q_y E}(ReZ_\perp) = 2.8 \times 10^{-2}\, Re(Z_\perp)\ \mathrm{sec}^{-1} \quad .$$

For $\tau > 500\ \mu$sec we need $Re(Z_\perp) \leq 71\ \mathrm{k}\Omega/\mathrm{m}$. This requirement may be difficult to meet. However, the beam can be stabilized by simply increasing the chromaticity $dQ_y/(dp/p)$ to -10 from its nominal value of -6.75.

7. Conclusion

These high-intensity machines do look feasible. If constructed, they would supply 12 times more beam power for producing spallation neutrons than the PSR design. A number of subjects still need to be addressed: collimator calculation, tracking, optimization, and a cost estimate.

Reference

1. R. J. Macek, D. H. Fitzgerald, R. L. Hutson, M. A. Plum, and H. A. Thiessen, Los Alamos National Laboratory Report LA-UR-88-1682 (1988).